

## Article

# Designing a Bayesian Regularization Approach to Solve the Fractional Layla and Majnun System

Zulqurnain Sabir <sup>1,2,\*</sup>, Atef F. Hashem <sup>3,4</sup> , Adnène Arbi <sup>5,6</sup>  and Mohamed A. Abdelkawy <sup>3,4</sup> 

- <sup>1</sup> Department of Mathematics and Statistics, Hazara University, Mansehra 21300, Pakistan
- <sup>2</sup> Department of Computer Science and Mathematics, Lebanese American University, Beirut 1401, Lebanon
- <sup>3</sup> Department of Mathematics and Statistics, College of Science, Imam Mohammad Ibn Saud Islamic University (IMSIU), Riyadh 13318, Saudi Arabia; affaragalla@imamu.edu.sa (A.F.H.); maohamed@imamu.edu.sa (M.A.A.)
- <sup>4</sup> Department of Mathematics and Information Science, Faculty of Science, Beni-Suef University, Beni-Suef 62514, Egypt
- <sup>5</sup> Laboratory of Engineering Mathematics (LR01ES13), Tunisia Polytechnic School, University of Carthage, Tunis 2078, Tunisia; adnen.arbi@enseignant.edunet.tn
- <sup>6</sup> Department of Advanced Sciences and Technologies at National School of Advanced Sciences and Technologies of Borj Cedria, University of Carthage, Hammam-Chott 1164, Tunisia
- \* Correspondence: zulqurnain\_maths@hu.edu.pk

**Abstract:** The present work provides the numerical solutions of the mathematical model based on the fractional-order Layla and Majnun model (MFLMM). A soft computing stochastic-based Bayesian regularization neural network approach (BRNNA) is provided to investigate the numerical accomplishments of the MFLMM. The nonlinear system is classified into two dynamics, whereas the correctness of the BRNNA is observed through the comparison of results. Furthermore, the reducible performance of the absolute error improves the exactitude of the computational BRNNA. Twenty neurons have been chosen, along with the data statics of training 74% and 13%, for both authorization and testing. The consistency of the designed BRNNA is demonstrated using the correlation/regression, error histograms, and transition of state values in order to solve the MFLMM.



**Citation:** Sabir, Z.; Hashem, A.F.; Arbi, A.; Abdelkawy, M.A. Designing a Bayesian Regularization Approach to Solve the Fractional Layla and Majnun System. *Mathematics* **2023**, *11*, 3792. <https://doi.org/10.3390/math11173792>

Academic Editor: Jonathan Blackledge

Received: 6 August 2023  
Revised: 30 August 2023  
Accepted: 30 August 2023  
Published: 4 September 2023



**Copyright:** © 2023 by the authors. Licensee MDPI, Basel, Switzerland. This article is an open access article distributed under the terms and conditions of the Creative Commons Attribution (CC BY) license (<https://creativecommons.org/licenses/by/4.0/>).

**Keywords:** Layla and Majnun; fractional; neural networks; Bayesian regularization approach; numerical solutions

**MSC:** 26A33; 68T07; 65C30

## 1. Introduction

Many Americans have claimed that psychology is the scientific study of the mind's active learning [1–3]. The mathematical connection in the modeling of love tales has rarely been conveyed to psychologists and scientists [4,5]. Manifestations of psychology have been observed in human growth, social environments, cognitive processes, and clinical behaviors [6,7]. A common psychological question about the meaning of love always comes to mind. Every person has their own justifications, with different meanings attached to them. Physical and spiritual love are the two main types of love. Physical love displays an inherent desire, whereas spiritual love is considered true as it does not alter depending on the circumstances. Someone who is experiencing love can occasionally become frightened and enraged. Those that are really in love have the sensation of the planet whirling. When someone falls in love, there is no discrimination based on creed, race, and religion. Feelings of love also occur in other creatures than humans. Romeo and Juliet, Sassi Punnuh, Heer Ranjha, Sohni Mahiwal, Haleema Ertugrul, and Layla Majnun are just a few examples of historical real-life love stories.

The current study displays the numerical results for the historical mathematical fractional Layla and Majnun model (MFLMM). This tale is so historic that Persia was aware of

it in the ninth century. The concepts of this tale have also been expressed in the languages of Pakistan, as well as in Persian, Arabic, Turkish, and Indian, among other languages. In addition to being described in the literature, this love story has also appeared in several film/drama industries. All religions preach love, whether it is the Torat, the Geeta, the Quran, or the Bible. No one can secure himself from love, either Khusro, Zuleka, Iqbal, Ghalib, or Bulay Shah.

These complex types of variables are implemented in numerous submissions, e.g., energy accelerators [8], optical systems [9], dynamical form of the rotor [10], plasma physics [11], complex damped system [12], and many more [13–15]. The current investigations calculate the solutions of the MFLMM by applying soft computing paradigms based on the Bayesian regularization neural network approach (BRNNA). The fractional derivatives are implemented in several real submissions [16,17]. The stochastic computing processes have been implemented in frequent applications including the nature of stiff, grim, singular, and complex differential models [18–20]. Some remarkable stochastic applications including food-chain nonlinear systems [21], coronavirus systems [22–24], biological HIV models [25], smoking differential systems [26], higher order singular systems [27], and delay systems [28]. But the stochastic BRNNA has never been applied before to solve the MFLMM. The novel characteristics of this study are presented as:

- The stochastic BRNNA is applied successfully for the numerical performances of the differential MFLMM.
- The fractional derivatives are implemented to accomplish the accurate performances of differential MFLMM.
- Three different variations based on the MFLMM are numerically simulated through the process of the BRNNA.
- The exactness of the BRNNA is perceived via comparison of performances-based achieved and source solutions.
- The reduceable absolute error (AE) performances authenticate the precision of the BRNNA for solving the MFLMM.
- The correlation/regression, error histograms (EHs), and transition of state (TS) values to solve the MFLMM demonstrate the reliability of the BRNNA.

The remaining parts of this work are as follows: Section 2 presents the MFLMM. Section 3 is the stochastic BRNNA. Section 4 represents the numerical MFLMM performances. Section 5 provides the concluding remarks.

## 2. Fractional LMM

The current section represents the MFLMM that is based on two relations, real and complex. The simplified model’s form including its two classes is shown as [29,30]:

$$\begin{cases} \frac{dM(\theta)}{d\theta} = \mu_a + \mu_c M(\theta) + L^2(\theta), & M_0 = k_1, \\ \frac{dL(\theta)}{d\theta} = \mu_b + \mu_d L(\theta) + M^2(\theta), & L_0 = k_2, \end{cases} \quad (1)$$

where  $\mu_a, \mu_b, \mu_c,$  and  $\mu_d$  are constants, while the initial conditions are  $k_1$  and  $k_2$ . Layla and Majnun’s feeling are stated as  $L(\theta)$  and  $M(\theta)$ . The parameter constants are represented as  $\mu_a$  and  $\mu_b$  based on the environmental spirits properties.  $\mu_a$  is a positive fixed value that shows the compassion and sympathy for Majnun, while  $\mu_b < 0$  represents the cruel people’s behavior towards Layla.  $L^2$  and  $M^2$  represent the extreme level of love.  $\mu_b < 0$  and  $\mu_d < 0$  are the emotions of real love. The simplified form of system (1) using the complex forms, i.e.,  $M = iM_i + M_r$  and  $L = iL_i + L_r$  is given as [31,32]:

$$\begin{cases} \frac{d}{d\theta} M_r(\theta) = \mu_c M_r(\theta) + \mu_a - L_i^2(\theta) + L_r^2(\theta), & (M_r)_0 = k_1, \\ \frac{d}{d\theta} M_i(\theta) = M_i(\theta)\mu_c + 2L_i(\theta)L_r(\theta), & (M_i)_0 = k_2, \\ \frac{d}{d\theta} L_r(\theta) = \mu_b + \mu_d L_r(\theta) - M_i^2(\theta) + M_r^2(\theta), & (L_r)_0 = k_3, \\ \frac{d}{d\theta} L_i(\theta) = \mu_d L_i(\theta) + 2M_i(\theta)M_r(\theta), & (L_i)_0 = k_4, \end{cases} \quad (2)$$

where,  $L_i(\theta)$  and  $M_i(\theta)$  are the emotions of Layla and Majnun based on the imaginary values, while  $L_r(\theta)$  and  $M_r(\theta)$  are the real emotions of these two characters. The subject of this study is to solve the MFLMM through the soft computing BRNNA. The nonlinear MFLMM is shown as [33]:

$$\begin{cases} D^\alpha M_r(\theta) = \mu_a + \mu_c M_r(\theta) - L_i^2(\theta) + L_r^2(\theta), & (M_r)_0 = k_1, \\ D^\alpha M_i(\theta) = \mu_c M_i(\theta) + 2L_i(\theta)L_r(\theta), & (M_i)_0 = k_2, \\ D^\alpha L_r(\theta) = \mu_b + \mu_d L_r(\theta) - M_i^2(\theta) + M_r^2(\theta), & (L_r)_0 = k_3, \\ D^\alpha L_i(\theta) = L_i(\theta)\mu_d + 2M_r(\theta)M_i(\theta), & (L_i)_0 = k_4. \end{cases} \quad (3)$$

In the above model,  $\alpha$  shows the Caputo derivative. The fractional derivatives are presented to accomplish the specific and accurate outcomes. The examination of minute features in fractional models are not easy to manage, but applying the integer kinds reveals more information about the system’s dynamics. In terms of proficiency, the fractional derivatives outperformed those based on the integer kind when the requirement was attainable [34,35]. Additionally, many applications that emerge in control networks, engineering, and mathematical systems have been used to solve the fractional derivatives [36–38]. Over the last 30 years, considerable operators have been used to solve various models [39,40]. Some of them are Riemann–Liouville, Caputo, Erdlyi–Kober, Grünwald–Letnikov and Weyl–Riesz [41,42]. Each of these operators has its own specific effects, but on the other hand, the Caputo derivative is considered easy to apply and can be implemented for the non-homogeneous/homogeneous initial conditions. The authors are encouraged to achieve the numerical performances of the MFLMM through the BRNN by keeping in view the significance of these submissions.

### 3. Designed Methodology

In this section, the methodology, based on the proposed BRNNA, for solving the differential MFLMM including the essential practices of the scheme and its execution is presented. The optimization based on the BRNNA is presented in Figure 1, which is categorized into MFLMM and model presentations.

In mathematical theory, there are various innovations based on supervised neural networks, which have contributed to understanding of training, behavior, and performance. Some of them are universal calculation depth and theorem, gradient descent and backpropagation, optimization surfaces and loss landscapes, generalization theory, weight initialization, normalization schemes, regularization and dropout, margin theory and loss functions, adaptive learning rates and schedules, network pruning and compression, Bayesian neural networks, elastic net, and weight regularization. These revolutions in mathematical theory have progressed the recognizing of supervised neural networks and have to more efficient training schemes, better system interpretability, and improved generalization. To create the dataset, the numerical performances are obtained by using the values of the default parameters. Twenty neurons are chosen, along with the data statics of training 74% and 13%, for the testing and certification. The stochastic BRNNA are presented using the best relationship, including premature convergence, complexity, and underfitting and overfitting measures. The program’s settings are also changed through understanding, simulations, training, and minor link inconsistencies. The designed BRNNA is applied in

“Matlab” with command “nftool” to achieve the assortment of learning schemes, proper hidden neurons, and certification/testing actions.

The computing performances have been achieved by using the BRNNA for the differential MFLMM. The same data need not necessarily be chosen for validation, training, and testing. Due to biased input outputs, the training is selected to be >74% to obtain the enhanced and superior appearances. If the training data are <74%, then the accuracy of the proposed BRNNA is reduced. Therefore, it is important to select these values with care and concentration. Figure 2 presents the different layers structure.

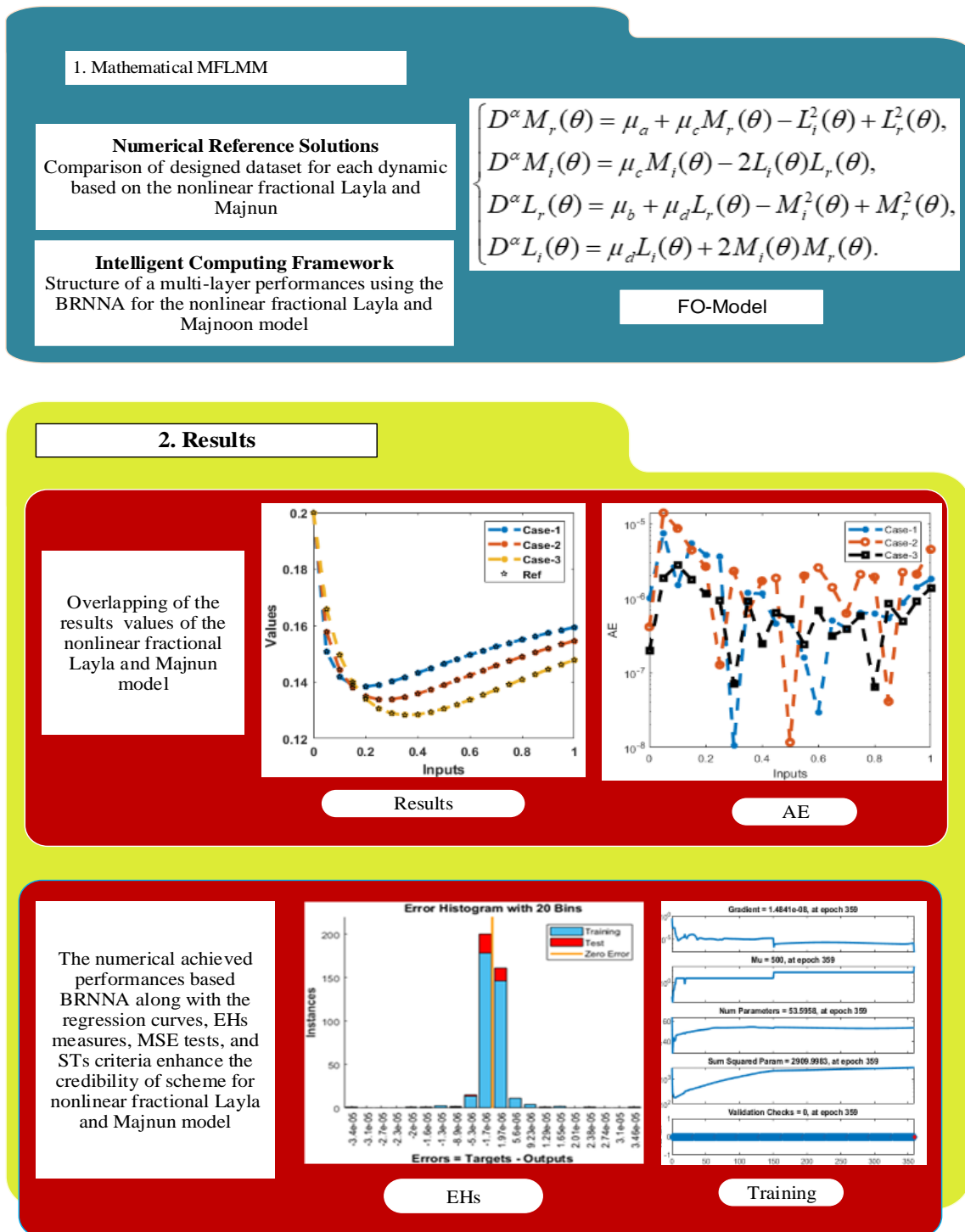
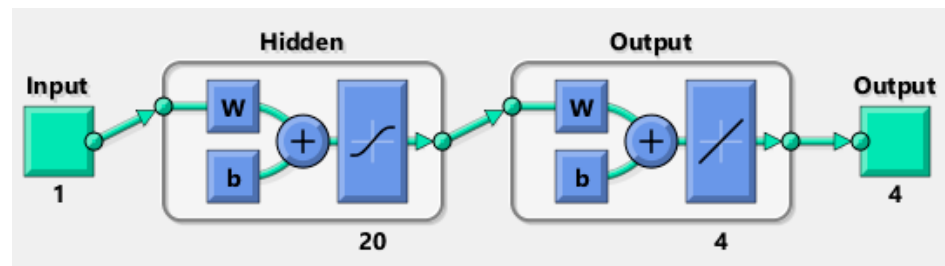


Figure 1. Depictions of the BRNNA for the MFLMM.



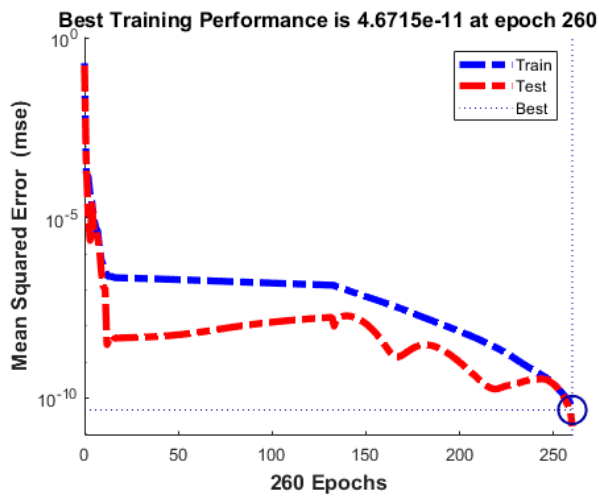
**Figure 2.** Different layer presentations for the MFLMM.

#### *Bayesian Regularization (BR) Scheme*

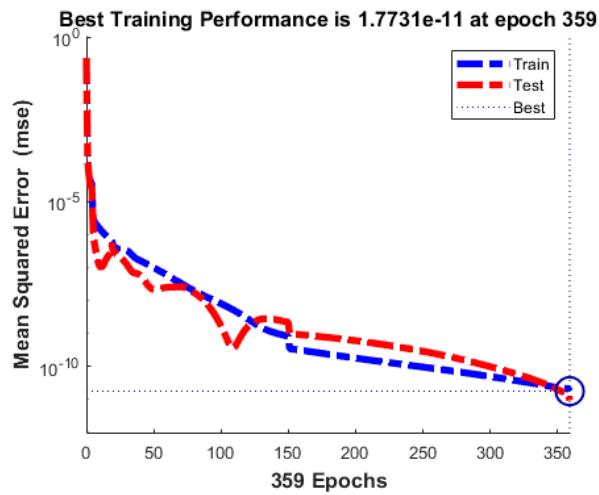
As compared to other traditional backpropagation approaches, one optimization technique that exhibits reliable and operational solutions is called BR. Cumbersome validation criteria are removed by using the BR. Many mathematical models have described the BR, which transforms regression representations into the constrained predictive method based on regression analysis. BR is an approach that is applied in statistics and machine learning to address uncertainty and overfitting by combining previous knowledge on the model's parameters. BR is commonly used in such scenarios as limited data or balancing the trade-off between data fitting and averting overly complicated systems. BR suggests a principled pathway to control system complexity, combine previous knowledge, and account for ambiguity in the statistical and machine learning tasks. Currently, BR is functional for applications such as making things measurable by exposure map rebuilding [43], the sensorless quantity of pumps [44], inverse acoustic systems [45], certification of groundwater pollution foundations along with hydraulic restrictions [46], economic systems [47], and permeability calculations based on the tight gas sandstones [48].

#### **4. Numerical Performances**

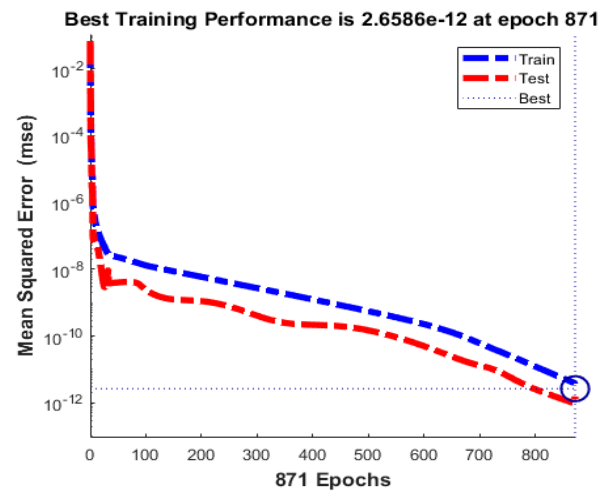
The current section provides three different cases by fixing these values  $\mu_d = -1$ ,  $\mu_b = -1$ ,  $\mu_a = 1$ , and  $\mu_c = -1$ , while the values of  $\alpha$  are taken as 0.6, 0.7 and 0.8. Figures 3–7 display the numerical MFLMM based on the designed BRNNA. Figures 3–5 present the MFLMM, which is developed using the computational BRNNA. The mean square error (MSE) results achieved by employing the BRNNA to solve the MFLMM are presented in Figure 3. The optimal results are presented as  $4.67150 \times 10^{-11}$ ,  $1.77309 \times 10^{-11}$ , and  $2.65858 \times 10^{-12}$  by using the epochs as 260, 359, and 871 for cases 1–3. By increasing the epochs, the testing, training, and endorsement curves perform the position of steady state using the performances up to  $10^{-12}$ . The gradient operator values for the first to the third case are presented as  $5.1178 \times 10^{-8}$ ,  $1.4841 \times 10^{-8}$ , and  $9.1037 \times 10^{-9}$ . An error gradient shows the magnitude and direction values that are performed during the process of training based on the proposed neural network, which is applied to enhance the weights of the network with the right amount and direction. Figure 4 shows the obtained calculated results along with the EHs measures to solve the MFLMM. The EHs for cases 1 to 3 of the MFLMM have been performed as  $1.81 \times 10^{-7}$ ,  $1.97 \times 10^{-6}$ , and  $6.45 \times 10^{-7}$ . Figure 4 shows a plot, based on justification, of the testing, and training that perform the best. It also shows the training that performs the momentum constant or parameter, which is contained in the updated weight expression to evade the local minimum issues. Figure 5 depicts the correlation graphs produced through the BRNNA for the MFLMM, which is one (perfect value) for each case. The coefficient of correlation ( $R$ ) varies in input  $-1$  and  $+1$ ; however, if  $R$  performance is found to be  $+1$ , high performance of the network is obtained along with positive linear relationship. The precision of the designed BRNNA for the MFLMM is achieved in the form of test/train and verification. Table 1 performs the MSE by using the BRNNA for the MFLMM.



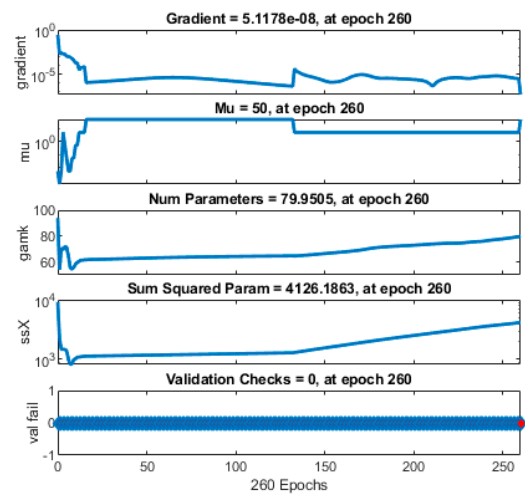
(a) Best authorization (1)



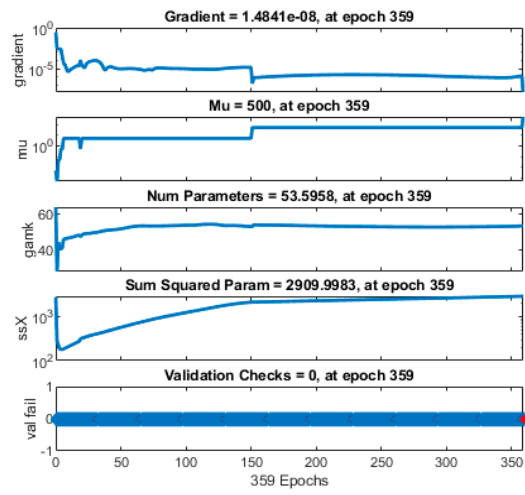
(b) Best authorization (2)



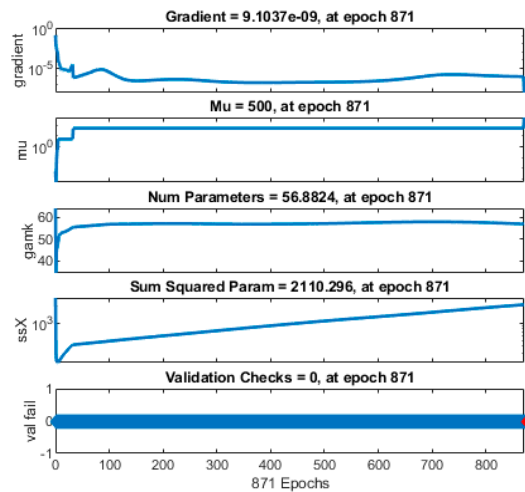
(c) Best authorization (3)



(d) Gradient (1)

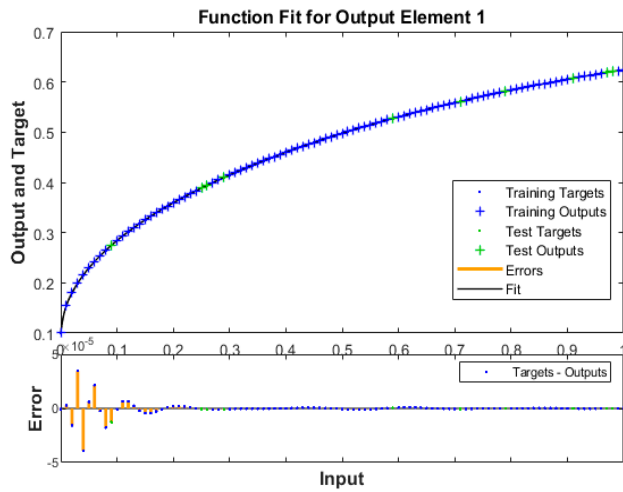


(e) Gradient (2)

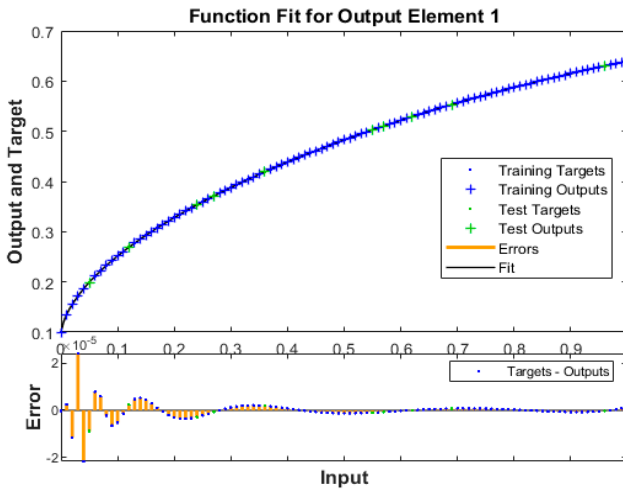


(f) Gradient (3)

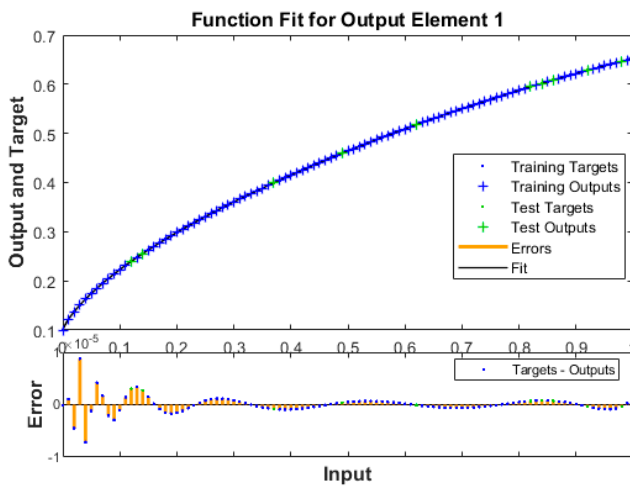
Figure 3. Best authorization and gradient values for the MFLMM.



(a) Fit funt (1)



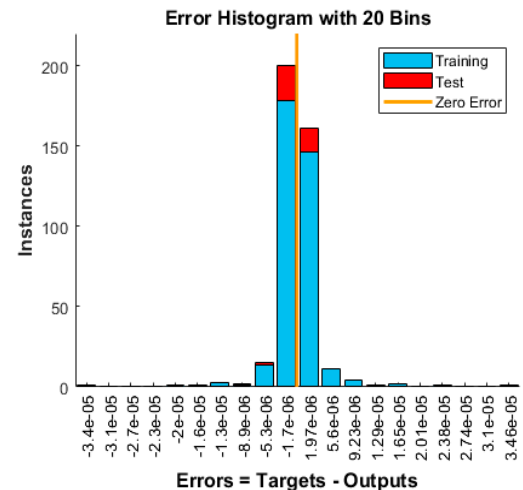
(b) Fit Func (2)



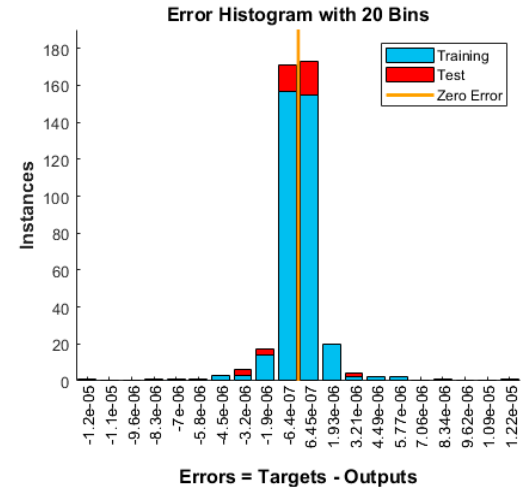
(c) Fit func (3)



(d) EHs (1)

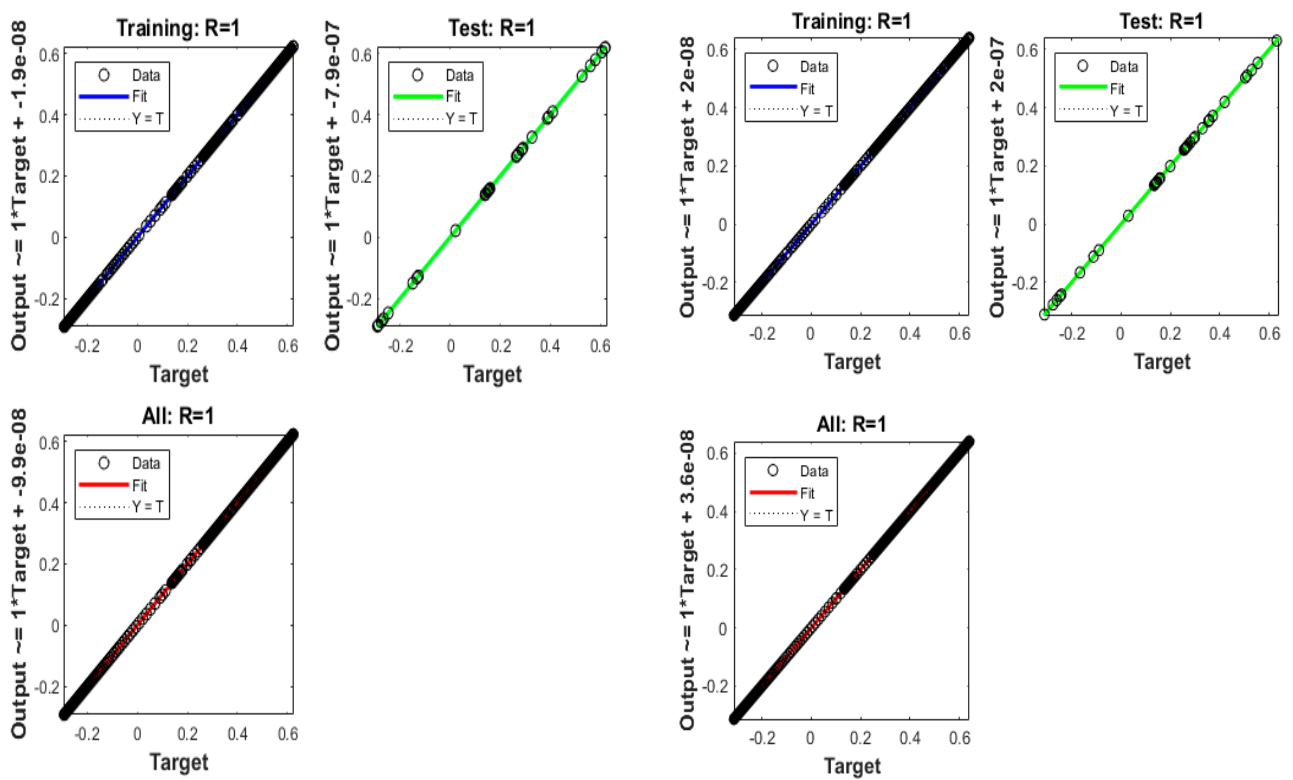


(e) EHs (2)



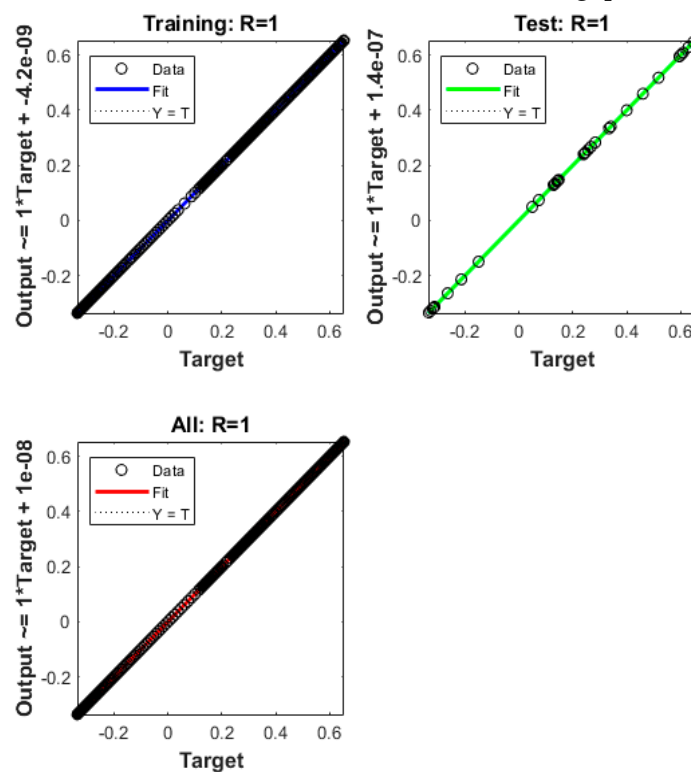
(f) EHs (3)

Figure 4. Fit function and EHs for MFLMM using the BRNNA.



(a) Reg. performance for case 1

(b) Reg. performance for case 2



(c) Reg. performance for case 3

Figure 5. Reg. measures for the MFLMM using the BRNNA.

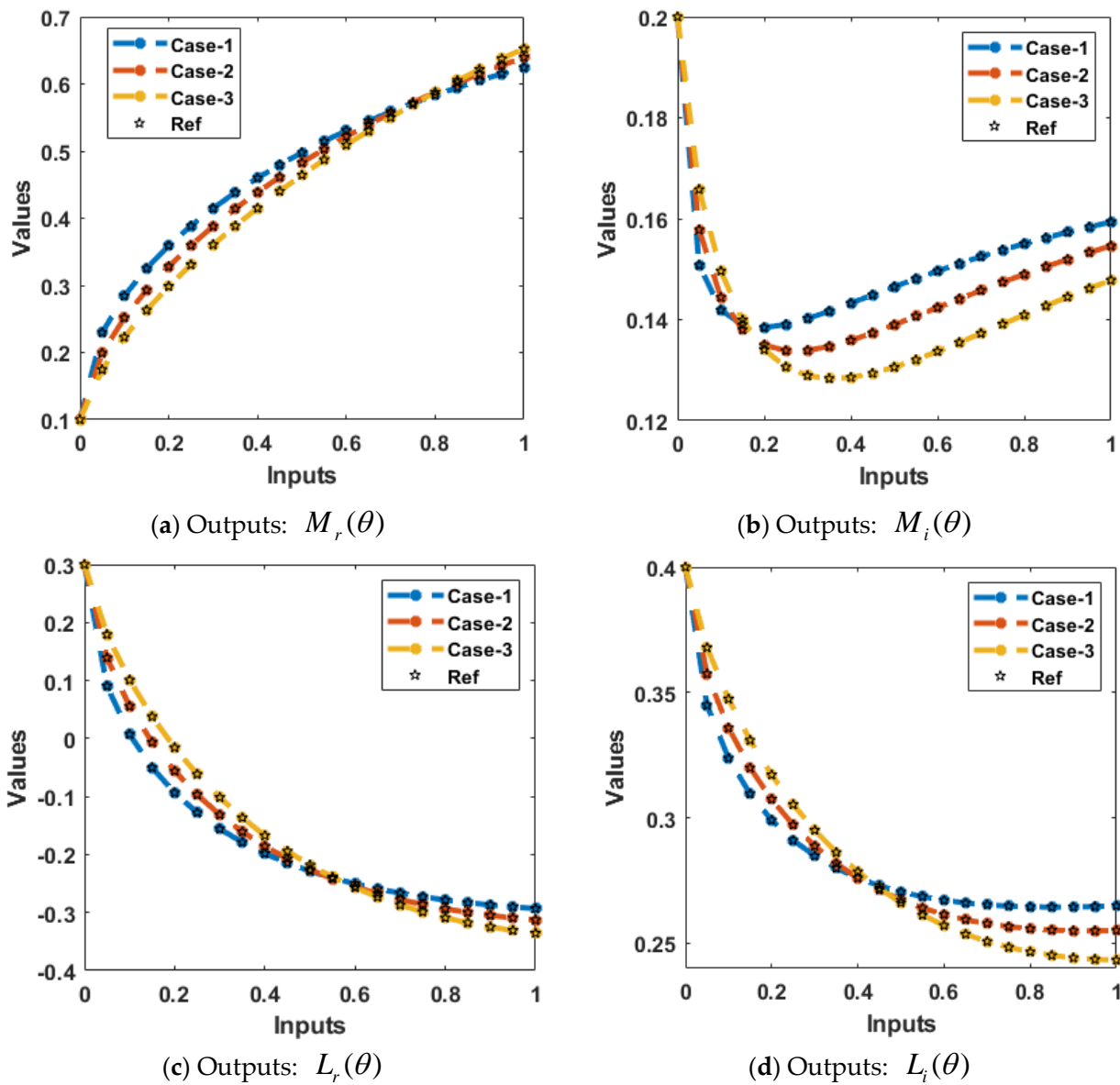


Figure 6. Result comparison for each class of the MFLMM using the BRNNA.

Figures 6 and 7 present the comparisons and the AE performances for the MFLMM using the BRNNA. Figure 6 provides the graphs of result comparisons that have been obtained through the matching of proposed and reference results. These corresponding results provide the accuracy of the scheme for solving the MFLMM. Figure 7 indicates the AE performances for each dynamic of the MFLMM. AE performances for  $M_r(\theta)$  are illustrated in Figure 7a, and lie as  $10^{-6}$ – $10^{-8}$ ,  $10^{-5}$ – $10^{-7}$ , and  $10^{-6}$ – $10^{-7}$  for cases 1 to 3. For the class  $M_i(\theta)$ , the AE for cases 1 to 3 is performed as  $10^{-5}$ – $10^{-6}$ ,  $10^{-5}$ – $10^{-7}$ , and  $10^{-6}$ – $10^{-7}$ . These measures for the classes  $L_r(\theta)$  and  $L_i(\theta)$  are derived in Figure 7c,d that are performed as  $10^{-6}$ – $10^{-9}$ ,  $10^{-6}$ – $10^{-8}$  and  $10^{-7}$ – $10^{-8}$  for the first to the third case. These results match and are reduceable to AE, which implies the accuracy of the BRNNA for solving the MFLMM.

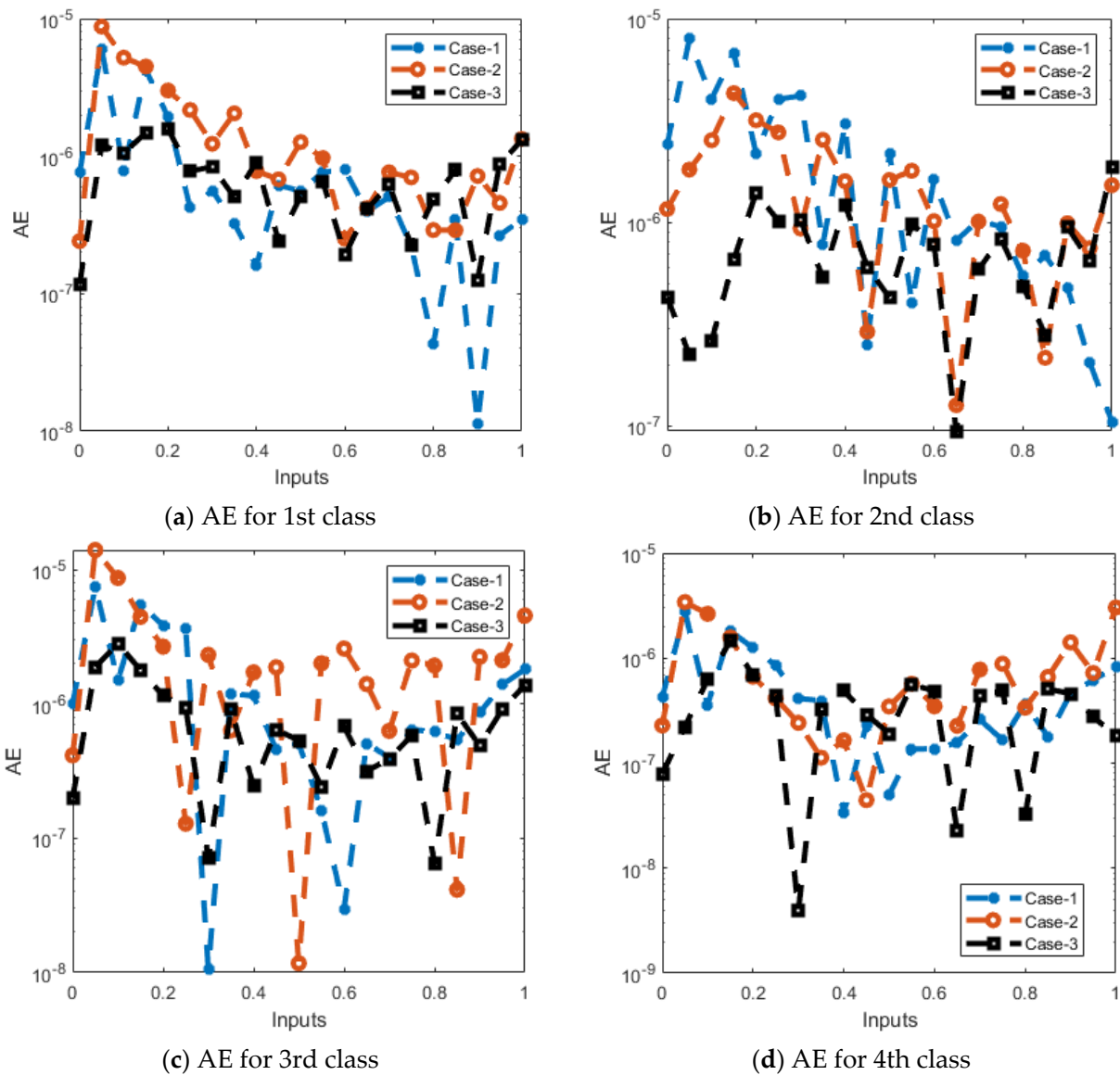


Figure 7. AE for the nonlinear dynamics based on the MFLMM.

Table 1. MSE performances through BRNNA for the MFLMM.

Case	MSE		Execution	Gradient	Epoch	Time
	Test	Train				
1	$1.65 \times 10^{-11}$	$4.67 \times 10^{-11}$	$4.67 \times 10^{-11}$	$5.12 \times 10^{-8}$	260	1 s
2	$9.35 \times 10^{-12}$	$1.65 \times 10^{-11}$	$1.77 \times 10^{-11}$	$1.48 \times 10^{-8}$	359	1 s
3	$1.55 \times 10^{-12}$	$2.65 \times 10^{-12}$	$2.66 \times 10^{-12}$	$9.10 \times 10^{-9}$	871	4 s

### 5. Concluding Remarks

The numerical representations using the artificial neural networks for solving the fractional-order mathematical Layla and Majnun system are provided in the current study. The mathematical nonlinear system is classified into two dynamics. A few concluding remarks of this study are:

- A soft computing Bayesian regularization-based neural network approach has been suggested successfully for the numerical representations of the MFLMM.
- For the accuracy of the results, the fractional derivatives have been provided to solve the mathematical model.

- The exactness of the proposed BRNNA has been validated through the overlapping of the results.
- The reducible absolute error performances improve the accuracy of the designed BRNNA.
- Twenty neurons have been selected, together with the statics of training 74% and 13%, for both certification and testing.
- The reliability and consistency of the designed BRNNA is demonstrated based on the correlation, transition of state, and performances of error histograms to solve the MFLMM.

In future work, this designed numerical BRNNA could be applied to solving various stiff nature models, including fractional love models [49,50], nonlinear fractional models [35], the Lonngren-wave equation [51], a Jeffrey fluid in contact with a Newtonian fluid [52], oscillation problems [53], quantum differential equations [54], the Bogoyavlensky–Konopelchenko model [55], and biological and fluid differential systems [35,43–55].

**Author Contributions:** Methodology, A.F.H. and M.A.A.; Software, Z.S.; Investigation, Z.S.; Data curation, A.F.H.; Writing—original draft, Z.S., A.A. and M.A.A.; Supervision, A.A. All authors have read and agreed to the published version of the manuscript.

**Funding:** This work was supported and funded by the Deanship of Scientific Research at Imam Mohammad Ibn Saud Islamic University (IMSIU) (grant number IMSIU-RP23088).

**Conflicts of Interest:** The authors declare that they have no conflict of interest.

## References

1. Jafari, S.; Ansari, Z.; Golpayegani, S.M.R.H.; Gharibzadeh, S. Is attention a “period window” in the chaotic brain? *J. Neuropsychiatry Clin. Neurosci.* **2013**, *25*, E05. [\[CrossRef\]](#)
2. Sprott, J.C. Dynamical models of happiness. *Nonlinear Dyn. Psychol. Life Sci.* **2005**, *9*, 23–36.
3. Baghdadi, G.; Jafari, S.; Sprott, J.C.; Towhidkhal, F.; Golpayegani, M.H. A chaotic model of sustaining attention problem in attention deficit disorder. *Commun. Nonlinear Sci. Numer. Simul.* **2015**, *20*, 174–185. [\[CrossRef\]](#)
4. Tabatabaei, S.S.; Yazdanpanah, M.J.; Jafari, S.; Sprott, J.C. Extensions in dynamic models of happiness: Effect of memory. *Int. J. Happiness Dev.* **2014**, *1*, 344–356. [\[CrossRef\]](#)
5. Farman, M.; Akgül, A.; Aldosary, S.F.; Nisar, K.S.; Ahmad, A. Fractional order model for complex Layla and Majnun love story with chaotic behaviour. *Alex. Eng. J.* **2022**, *61*, 6725–6738. [\[CrossRef\]](#)
6. Dercole, F.; Rinaldi, S. Love stories can be unpredictable: Jules et Jim in the vortex of life. *Chaos Interdiscip. J. Nonlinear Sci.* **2014**, *24*, 023134. [\[CrossRef\]](#) [\[PubMed\]](#)
7. Liao, X.; Ran, J. Hopf bifurcation in love dynamical models with nonlinear couples and time delays. *Chaos Solitons Fractals* **2007**, *31*, 853–865. [\[CrossRef\]](#)
8. Alves-Pires, R. *Nonlinear Dynamics in Particle Accelerators*; World Scientific: Singapore, 1996; Volume 23.
9. Newell, A.; Moloney, J. *Nonlinear Optics*; Addison-Wesley: Reading, MA, USA, 1992.
10. Cveticanin, L. Resonant vibrations of nonlinear rotors. *Mech. Mach. Theory* **1995**, *30*, 581–588. [\[CrossRef\]](#)
11. Rozhansky, V.A.; Tsandin, L.D. *Transport Phenomena in Partially Ionized Plasma*; CRC Press: Boca Raton, FL, USA, 2001.
12. Wu, X.; Xu, Y.; Zhang, H. Random impacts of a complex damped system. *Int. J. Non-Linear Mech.* **2011**, *46*, 800–806. [\[CrossRef\]](#)
13. Cveticanin, L. Approximate analytical solutions to a class of non-linear equations with complex functions. *J. Sound Vib.* **1992**, *157*, 289–302. [\[CrossRef\]](#)
14. Xu, Y.; Xu, W.; Mahmoud, G.M. On a complex beam–beam interaction model with random forcing. *Phys. A Stat. Mech. Appl.* **2004**, *336*, 347–360. [\[CrossRef\]](#)
15. Mahmoud, G.M.; Aly, S.A. On periodic solutions of parametrically excited complex non-linear dynamical systems. *Phys. A Stat. Mech. Its Appl.* **2000**, *278*, 390–404. [\[CrossRef\]](#)
16. Ghanbari, B.; Djilali, S. Mathematical and numerical analysis of a three-species predator-prey model with herd behavior and time fractional-order derivative. *Math. Methods Appl. Sci.* **2020**, *43*, 1736–1752. [\[CrossRef\]](#)
17. Sabir, Z.; Raja, M.A.Z.; Umar, M.; Shoaib, M.; Baleanu, D. FMNSICS: Fractional Meyer neuro-swarm intelligent computing solver for nonlinear fractional Lane–Emden systems. *Neural Comput. Appl.* **2022**, *34*, 4193–4206. [\[CrossRef\]](#)
18. Sabir, Z.; Nisar, K.; Raja, M.A.Z.; Ibrahim, A.A.B.A.; Rodrigues, J.J.; Al-Basyouni, K.S.; Mahmoud, S.R.; Rawat, D.B. Design of Morlet wavelet neural network for solving the higher order singular nonlinear differential equations. *Alex. Eng. J.* **2021**, *60*, 5935–5947. [\[CrossRef\]](#)
19. Sabir, Z.; Raja, M.A.Z.; Alnahdi, A.S.; Jeelani, M.B.; Abdelkawy, M.A. Numerical investigations of the nonlinear smoke model using the Gudermannian neural networks. *Math. Biosci. Eng.* **2022**, *19*, 351–370. [\[CrossRef\]](#) [\[PubMed\]](#)

20. Sabir, Z.; Wahab, H.A.; Javeed, S.; Baskonus, H.M. An Efficient Stochastic Numerical Computing Framework for the Nonlinear Higher Order Singular Models. *Fractal Fract.* **2021**, *5*, 176. [[CrossRef](#)]
21. Sabir, Z. Stochastic numerical investigations for nonlinear three-species food chain system. *Int. J. Biomath.* **2022**, *15*, 2250005. [[CrossRef](#)]
22. Umar, M.; Sabir, Z.; Raja, M.A.Z.; Amin, F.; Saeed, T.; Guerrero-Sanchez, Y. Integrated neuro-swarm heuristic with interior-point for nonlinear Sitr model for dynamics of novel COVID-19. *Alex. Eng. J.* **2021**, *60*, 2811–2824. [[CrossRef](#)]
23. Umar, M.; Sabir, Z.; Raja, M.A.Z.; Shoaib, M.; Gupta, M.; Sánchez, Y.G. A stochastic intelligent computing with neuro-evolution heuristics for nonlinear Sitr system of novel COVID-19 dynamics. *Symmetry* **2020**, *12*, 1628. [[CrossRef](#)]
24. Umar, M.; Sabir, Z.; Raja, M.A.Z.; Aguilar, J.G.; Amin, F.; Shoaib, M. Neuro-swarm intelligent computing paradigm for nonlinear HIV infection model with CD4+ T-cells. *Math. Comput. Simul.* **2021**, *188*, 241–253. [[CrossRef](#)]
25. Umar, M.; Sabir, Z.; Raja, M.A.Z.; Baskonus, H.M.; Yao, S.W.; İlhan, E. A novel study of Morlet neural networks to solve the nonlinear HIV infection system of latently infected cells. *Results Phys.* **2021**, *25*, 104235. [[CrossRef](#)]
26. Saeed, T.; Sabir, Z.; Alhodaly, M.S.; Alsulami, H.H.; Sánchez, Y.G. An advanced heuristic approach for a nonlinear mathematical based medical smoking model. *Results Phys.* **2022**, *32*, 105137. [[CrossRef](#)]
27. Sabir, Z.; Raja, M.A.Z.; Guirao, J.L.; Shoaib, M. Integrated intelligent computing with neuro-swarming solver for multi-singular fourth-order nonlinear Emden–Fowler equation. *Comput. Appl. Math.* **2020**, *39*, 307. [[CrossRef](#)]
28. Guirao, J.L.; Sabir, Z.; Saeed, T. Design and numerical solutions of a novel third-order nonlinear Emden–Fowler delay differential model. *Math. Probl. Eng.* **2020**, *2020*, 7359242. [[CrossRef](#)]
29. Jafari, S.; Sprott, J.C.; Golpayegani, S.M.R.H. Layla and Majnun: A complex love story. *Nonlinear Dyn.* **2016**, *83*, 615–622. [[CrossRef](#)]
30. Kumar, P.; Erturk, V.S.; Murillo-Arcila, M. A complex fractional mathematical modeling for the love story of Layla and Majnun. *Chaos Solitons Fractals* **2021**, *150*, 111091. [[CrossRef](#)]
31. Sabir, Z.; Said, S.B. A fractional order nonlinear model of the love story of Layla and Majnun. *Sci. Rep.* **2023**, *13*, 5402. [[CrossRef](#)]
32. Sabir, Z.; Baleanu, D.; Raja, M.A.Z.; Alshomrani, A.S.; Hincal, E. Computational performances of morlet wavelet neural network for solving a nonlinear dynamic based on the mathematical model of the affection of layla and majnun. *Fractals* **2023**, *31*, 2340016. [[CrossRef](#)]
33. Sabir, Z.; Guirao, J.L. A Soft Computing Scaled Conjugate Gradient Procedure for the Fractional Order Majnun and Layla Romantic Story. *Mathematics* **2023**, *11*, 835. [[CrossRef](#)]
34. Yokuş, A.; Gülbahar, S. Numerical solutions with linearization techniques of the fractional Harry Dym equation. *Appl. Math. Nonlinear Sci.* **2019**, *4*, 35–42. [[CrossRef](#)]
35. İlhan, E.; Kıymaz, İ.O. A generalization of truncated M-fractional derivative and applications to fractional differential equations. *Appl. Math. Nonlinear Sci.* **2020**, *5*, 171–188. [[CrossRef](#)]
36. Elsonbaty, A.M.R.; Sabir, Z.; Ramaswamy, R.; Adel, W. Dynamical analysis of a novel discrete fractional SITRS model for COVID-19. *Fractals* **2021**, *29*, 2140035. [[CrossRef](#)]
37. Mukdasai, K.; Sabir, Z.; Raja, M.A.Z.; Sadat, R.; Ali, M.R.; Singkibud, P. A numerical simulation of the fractional order Leptospirosis model using the supervise neural network. *Alex. Eng. J.* **2022**, *61*, 12431–12441. [[CrossRef](#)]
38. Yu, F. Integrable coupling system of fractional soliton equation hierarchy. *Phys. Lett. A* **2009**, *373*, 3730–3733. [[CrossRef](#)]
39. Bonilla, B.; Rivero, M.; Trujillo, J.J. On systems of linear fractional differential equations with constant coefficients. *Appl. Math. Comput.* **2007**, *187*, 68–78. [[CrossRef](#)]
40. Ibrahim, R.W.; Momani, S. On the existence and uniqueness of solutions of a class of fractional differential equations. *J. Math. Anal. Appl.* **2007**, *334*, 1–10. [[CrossRef](#)]
41. Diethelm, K.; Ford, N.J. Analysis of fractional differential equations. *J. Math. Anal. Appl.* **2002**, *265*, 229–248. [[CrossRef](#)]
42. Momani, S.; Ibrahim, R.W. On a fractional integral equation of periodic functions involving Weyl–Riesz operator in Banach algebras. *J. Math. Anal. Appl.* **2008**, *339*, 1210–1219. [[CrossRef](#)]
43. De Rochefort, L.; Liu, T.; Kressler, B.; Liu, J.; Spincemaille, P.; Lebon, V.; Wu, J.; Wang, Y. Quantitative susceptibility map reconstruction from MR phase data using bayesian regularization: Validation and application to brain imaging. *Magn. Reson. Med. Off. J. Int. Soc. Magn. Reson. Med.* **2010**, *63*, 194–206. [[CrossRef](#)] [[PubMed](#)]
44. Wu, D.; Huang, H.; Qiu, S.; Liu, Y.; Wu, Y.; Ren, Y.; Mou, J. Application of Bayesian regularization back propagation neural network in sensorless measurement of pump operational state. *Energy Rep.* **2022**, *8*, 3041–3050. [[CrossRef](#)]
45. Pereira, A.; Antoni, J.; Leclere, Q. Empirical Bayesian regularization of the inverse acoustic problem. *Appl. Acoust.* **2015**, *97*, 11–29. [[CrossRef](#)]
46. Pan, Z.; Lu, W.; Fan, Y.; Li, J. Identification of groundwater contamination sources and hydraulic parameters based on bayesian regularization deep neural network. *Environ. Sci. Pollut. Res.* **2021**, *28*, 16867–16879. [[CrossRef](#)]
47. Kiani, A.K.; Khan, W.U.; Raja, M.A.Z.; He, Y.; Sabir, Z.; Shoaib, M. Intelligent backpropagation networks with bayesian regularization for mathematical models of environmental economic systems. *Sustainability* **2021**, *13*, 9537. [[CrossRef](#)]
48. Zhou, Y.; Zhao, X.; Jiang, C.; Liu, S.; Han, Z.; Wang, G. Permeability prediction of multi-stage tight gas sandstones based on Bayesian regularization neural network. *Mar. Pet. Geol.* **2021**, *133*, 105320. [[CrossRef](#)]
49. Huang, L.; Bae, Y. Chaotic dynamics of the fractional-love model with an external environment. *Entropy* **2018**, *20*, 53. [[CrossRef](#)]

50. Huang, L.; Bae, Y. Nonlinear behavior in fractional-order Romeo and Juliet's love model influenced by external force with fuzzy function. *Int. J. Fuzzy Syst.* **2019**, *21*, 630–638. [[CrossRef](#)]
51. Baskonus, H.M.; Bulut, H.; Sulaiman, T.A. New complex hyperbolic structures to the lonngren-wave equation by using sine-gordon expansion method. *Appl. Math. Nonlinear Sci.* **2019**, *4*, 141–150. [[CrossRef](#)]
52. Vajravelu, K.; Sreenadh, S.; Saravana, R. Influence of velocity slip and temperature jump conditions on the peristaltic flow of a Jeffrey fluid in contact with a Newtonian fluid. *Appl. Math. Nonlinear Sci.* **2017**, *2*, 429–442. [[CrossRef](#)]
53. Selvi, M.S.M.; Rajendran, L. Application of modified wavelet and homotopy perturbation methods to nonlinear oscillation problems. *Appl. Math. Nonlinear Sci.* **2019**, *4*, 351–364. [[CrossRef](#)]
54. Gençoğlu, M.T.; Agarwal, P. Use of quantum differential equations in sonic processes. *Appl. Math. Nonlinear Sci.* **2021**, *6*, 21–28. [[CrossRef](#)]
55. Baskonus, H.M.; Senel, M.; Kumar, A.; Yel, G.; Senel, B.; Gao, W. On the Wave Properties of the Conformable Generalized Bogoyavlensky—Konopelchenko Equation. In *Handbook of Fractional Calculus for Engineering and Science*; Chapman and Hall/CRC: Boca Raton, FL, USA, 2022; pp. 103–119.

**Disclaimer/Publisher's Note:** The statements, opinions and data contained in all publications are solely those of the individual author(s) and contributor(s) and not of MDPI and/or the editor(s). MDPI and/or the editor(s) disclaim responsibility for any injury to people or property resulting from any ideas, methods, instructions or products referred to in the content.